Monofractal or multifractal: a case study of spatial distribution of mining-induced seismic activity

M. Eneva

Nonlinear Processes in Geophysics (1994) 1: 182 - 190

Nonlinear Processes in Geophysics

Monofractal of multifractal: a case study of spatial distribution of mining induced seismic activity

M. Eneva

Department of Physics/Geophysics, University of Toronto, 60 St. George Street, Toronto, Ontario, Canada M5S 1A7

Received 6 December 1993 - Accepted 22 April 1994 - Communicated by D. Sornette

Abstract. Using finite data sets and limited size of study volumes may result in significant spurious effects when estimating the scaling properties of various physical processes. These effects are examined with an example featuring the spatial distribution of induced seismic activity in Creighton Mine (northern Ontario, Canada). The events studied in the present work occurred during a three-month period, March-May 1992, within a volume of approximate size 400 x 400 x 180 m^3. Two sets of microearthquake locations are studied: Data Set 1 (14,338 events) and Data Set 2 (1654 events). Data Set 1 includes the more accurately located events and amounts to about 30 per cent of all recorded data. Data Set 2 represents a portion of the first data set that is formed by the most accurately located and the strongest microearthquakes.

The spatial distribution of events in the two data sets is examined for scaling behaviour using the method of generalized correlation integrals featuring various moments q. From these, generalized correlation dimensions are estimated using the slope method. Similar estimates are made for randomly generated point sets using the same numbers of events and the same study volumes as for the real data. Uniform and monofractal random distributions are used for these simulations. In addition, samples from the real data are randomly extracted and the dimension spectra for these are examined as well.

The spectra for the uniform and monofractal random generations show spurious multifractality due only to the use of finite numbers of data points and limited size of study volume. Comparing these with the spectra of dimensions for Data Set 1 and Data Set 2 allows us to estimate the bias likely to be present in the estimates for the real data. The strong multifractality suggested by the spectrum for Data Set 2 appears to be largely spurious; the spatial distribution, while different from uniform, could originate from a monofractal process. The spatial distribution of microearthquakes in Data Set 1 is either monofractal as well, or only weakly multifractal. In all similar studies, comparisons of results from real data and simulated point sets may help distinguish between genuine and artificial multifractality, without necessarily resorting to large numbers of data.

1 Introduction

A number of methods have been applied in recent years to quantitatively analyze structures in geophysical systems whose behaviour is best described as non-linear. The concepts of simple self-similarity and monofractals came to be widely used. Some of the geophysical phenomena to which monofractal distributions have been applied are crustal fragmentation (e.g., Aviles and Scholz, 1987; Turcotte, 1986), size distribution of earthquakes (e.g., Aki, 1981; Rundle, 1989), spatial distribution of earthquakes (e.g., Kagan and Knopoff, 1980; Hirata, 1989; Eneva, 1994; Henderson and Main, 1992; Main, 1992), and mining induced microearthquakes (Coughlin and Kranz, 1991; Eneva and Young, 1993).

At present, the notion of monofractals appears insufficient in many cases to address the richness of non-linear behaviour. The natural framework for scale-invariant non-linear dynamic systems seems to be better described by multifractals (e.g., Grassberger, 1983; Hentschel and Procaccia, 1983; Halsey et al., 1986; Pawelzik and Schuster, 1987). Some of the various applications of multifractals have been in the fields of astrophysics (e.g., Atmanspacher et al., 1988); physics of atmosphere, rain, and clouds (e.g., Lovejoy and Schertzer, 1990; Tessier et al., 1993); sediment studies (e.g., Block et al., 1991); crustal faulting (Davy et al., 1992); and earthquakes (Hirata and Imoto, 1991).

Among various methods to evaluate the fractal dimension when simple invariance is assumed, the correlation integral method has been particularly widely

used (Grassberger and Procaccia, 1983). In this method, the correlation dimension is estimated as the slope of the straight segment of the correlation integral C(r) in a double-logarithmic plot, log(C(r))-log(r), where r is distance and C(r) is number of pairs of points with distances smaller than r. The notion of correlation dimension has been extended to generalized correlation dimensions (e.g., Grassberger, 1983; Hentschel and Procaccia, 1983) featuring various moments q of the correlation integral; the generalized correlation dimension for q=2 is the standard correlation dimension. The generalized correlation dimensions have been used to evaluate the global scaling properties displayed by various experimental data sets (e.g., Block et al., 1991; Atmanspacher et al., 1988; Kurths and Herzel, 1987; Hirata and Imoto, 1991).

Theoretically, the spectra of generalized dimensions for different moments q have specific characteristics for multifractals, while no dependence on q is expected for monofractals. On the basis of this, with few exceptions (e.g., Block et al., 1991; Marshak et al., 1993), multifractality has been assumed in various studies as soon as the spectra of dimensions estimated from the experimental data appeared to have the shape expected for multifractals. The problem with such assumptions is that the experimental data sets feature certain measurement errors and are always finite, in terms of numbers of data points and size of study volume. This can result in spurious multifractality in the estimated spectra. As the generalized correlation integrals naturally show saturation for large distances, it has been frequently assumed that estimates below the points of saturation are essentially free of the edge effect for limited data sets. In fact, the existence of statistically good straight segments (scaling regions) in the correlation integrals still does not mean that these segments are unaffected by saturation and other factors. For this reason, the estimates of the correlation dimensions can be quite low and since the effect of finite data sets varies for different moments, monofractals may appear as multifractals.

In the present work the slope method using the generalized correlation integrals is applied to the spatial distribution of seismic activity induced in mines. The particular data used here originates from Creighton Mine, a copper-nickel mine near Sudbury, northern Ontario (Canada). Previous work with earthquake catalogues from various seismically active areas (e.g., Eneva et al., 1992; Eneva, 1994) suggested that the spatial distribution of seismic events is in many ways more informative than their temporal distribution. This motivated the emphasis on spatial distribution in the case of mining induced seismicity as well (Eneva and Young, 1993). Particular attention is payed here to the effect of limited data sets on the estimates of the global scaling properties. This effect has important implications for the conclusions one can derive from all similar studies, as well as for the practical use of the parameters estimated. It is noteworthy that these estimates can be effectively used even in the presence of significant bias due to the finite data sets. This is possible through comparison of the results from the real data with estimates from randomly generated sets of points with the same limitations as the real data. Since the underlying distributions for the randomly generated sets are known (uniform and monofractal distributions are used here), the edge effect can be readily evaluated for such simulations. This allows us to estimate the errors committed when the real data sets are studied.

2 Data

The data used in this work was supplied by Inco Ltd., the owner of Creighton Mine. The study period is March-May 1992. Creighton Mine is characterized by the highest level of seismic activity among all the nine nickel-copper mines operated by Inco Ltd. in the Sudbury Basin of northern Ontario; more than 46,000 events were recorded in this mine during the three-month study period. The excavation process is quite intensive, as evidenced by more than 400 blasts during the same period. Rockburst concerns have been high here, especially after a particularly damaging M3.6 event in 1987 (Morrison and MacDonald, 1990). 'Rockburst' is a mining term to indicate an event causing more damage than certain preset criteria.

The study volume is relatively small, about 400 x 400 x 180 m^3 in size. It is located below 2 km depth. A dense array of 64 receivers of the so-called MP-250 systems encompasses this small volume. Magnitude estimates are not available for the events recorded by this array. The sizes of the largest events, however, are known, as events of magnitudes above 1.5 are completely recorded by the local and regional seismic networks. Seven such events occurred in and around the study volume during the three-month period, the strongest of those being a M2.6 rockburst. Thus, the majority of events featured in the present work are microearthquakes with unknown magnitudes; had their magnitudes been measured, many of them would be negative.

The data used here consists of microearthquake locations obtained by using an algorithm specifically designed to work with the arrivals recorded by the MP-250 systems (Ge and Kaiser, 1990). The range 8-15 m is probably representative for the lower limit of the location accuracy for this data (Eneva and Young, 1993). Only the more accurately located events were used for the present study. Data Set 1 includes 14,338 microearthquake locations (30% of all located events). Although magnitudes for these events are largely unknown, a special ranking procedure (Ge and Kaiser, 1990) allows us to assume which of the microearthquakes may be the strongest ones. Thus, Data Set 2 (1654 events) includes

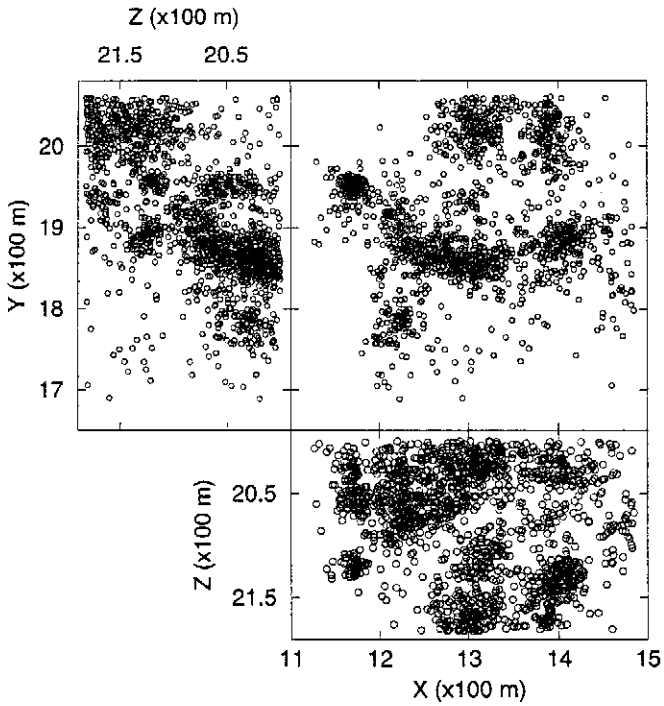

Fig.1. Microearthquake locations for Data Set 2 (Creighton Mine, March-May, 1992): horizontal plane and two vertical cross-sections, (x,y), (z,y) and (x,z), respectively; x, y, and z are mine co-ordinates.

about 1/9 of Data Set 1 and consists of the most accurately located and the strongest events (Fig.1). The same study volume (size above) was used to extract the events in both data sets. While the events in Data Set 1 fill in the entire volume, the effective volume covered by Data Set 2 is smaller, not more than 85% of the initially imposed study volume; a difference that will play an important role for understanding the results in this work.

3 Technique

The global scaling properties of the two data sets are evaluated using the so-called generalized correlation dimensions $D^{(q)}$ (e.g., Grassberger, 1983; Hentschel and Procaccia, 1983). These are evaluated as the slopes of the straight segments displayed by the generalized correlation integrals (e.g., Pawelzik and Schuster, 1987; Kurths and Herzel, 1987; Atmanspacher et al., 1988) in double-logarithmic plots. The generalized correlation integrals are given by:

$$C^{(q)}(r) = \lim_{r \to 0} \left[\frac{1}{N} \sum_{i=1}^{N} \left[\frac{1}{N} \sum_{j=1}^{N} \theta\left(r - |x_i - x_j|\right) \right]^{q-1} \right]^{1/(q-1)} \qquad (1)$$

The Heaviside function Θ above counts how many pairs of points (x_i, x_j) fall within distance r. The spectrum of dimensions $D^{(q)}$ can be used to evaluate the distribution for multifractal behaviour. q=0, 1, and 2, correspond to the better known capacity (or fractal), information, and correlation dimensions, respectively.

Figure 2 shows schematically the $D^{(q)}$-spectrum for a hypothetical data set characterized by a multifractal behaviour. In contrast, a monofractal is characterized by the same dimensions for all values of the moment q; i.e., the spectrum $D^{(q)}$ ideally turns into a horizontal line. The special cases of uniform random distribution of points on a plane or in a volume would be indicated in Fig.2 by a $D^{(q)}$-spectrum that is a horizontal line through the values of 2 or 3, respectively. It is repeatedly emphasized further that this will not be observed unless the number of points considered and the size of the volume in which these points are distributed are infinite for all practical purposes. Otherwise, the spectrum may exhibit a spurious multifractal behaviour for both monofractal and uniform random point sets. One cannot then reliably conclude that a finite data set is characterized by a genuine multifractal behaviour only because the $D^{(q)}$-spectrum exhibits a shape expected for multifractals. In view of this, the scaling properties of the spatial distribution of mining induced seismicity are evaluated not only for the real data, but also for simulated points that are randomly generated by using uniform and monofractal distributions.

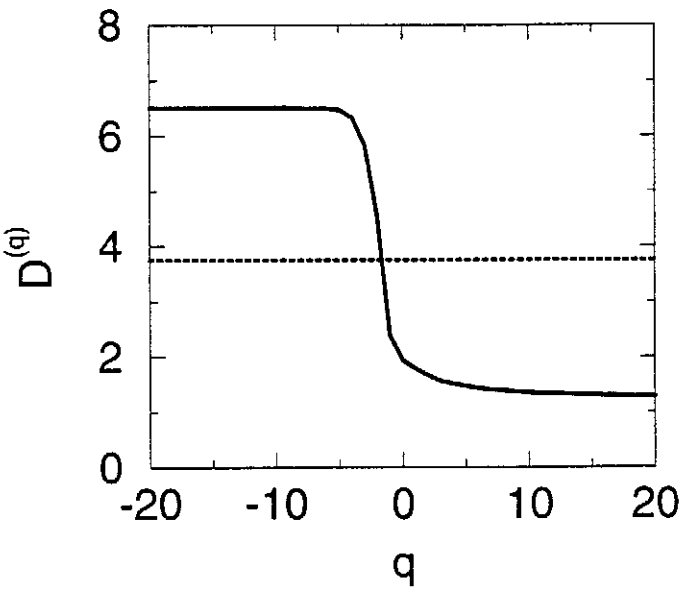

Fig.2. Schematic representation of the $D^{(q)}$-spectra for multifractals (solid line) and monofractals (dotted line).

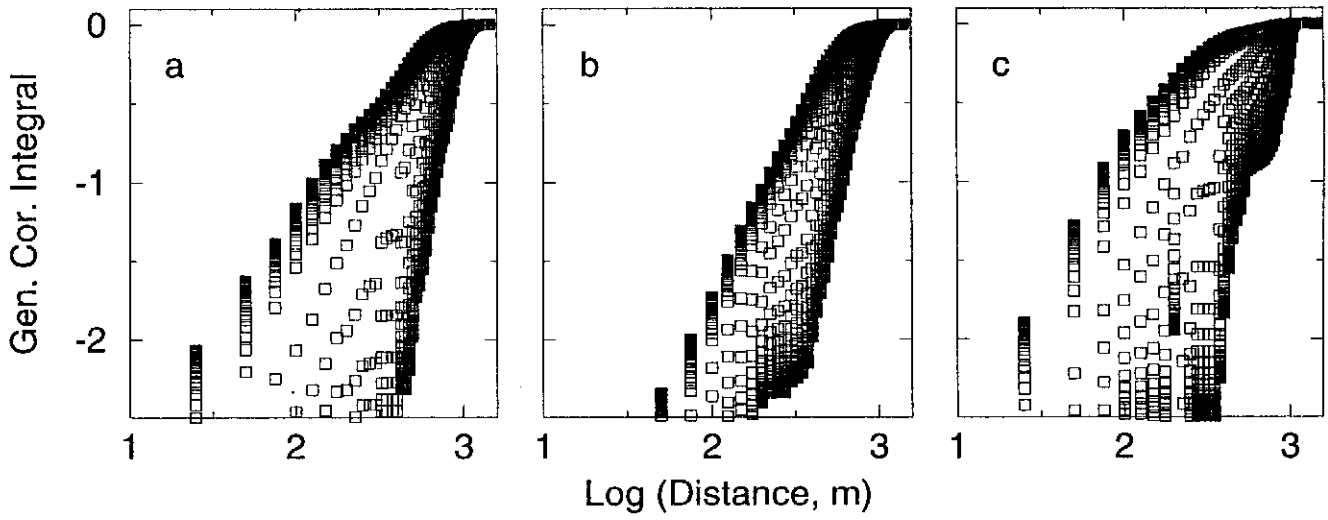

Fig.3. Generalized correlation integrals for: (a) Data Set 2 (1654 events); (b) 1654 randomly generated points using a uniform distribution; (c) 1654 randomly generated points using a monofractal distribution with fractal dimension 2.35. Generalized correlation integrals from right to left of each plot are calculated for q changing from -25 to 25 with step 1.

4 Results

4.1 Correlation integrals for Data Set 2 and simulated point sets

Figure 3a shows the correlation integrals $D^{(q)}(r)$ for Data Set 2 (1654 events), obtained using Eq.(1) for integer values of q between -25 and 25. If the effect of using limited data sets can be ignored, the "spreading" pattern observed would be indicative for a multifractal behaviour. However, the two remaining frames in Fig.3 show that this effect has to be accounted for in the case studied here. The generalized correlation integrals in these frames are obtained from 1654 randomly generated points using two different distributions: uniform (Fig.3b) and monofractal (Fig.3c). Uniform random distribution is used in order to compare the generalized correlation integrals obtained from the real data (Fig.3a) with the integrals from points occurring with equal probability everywhere in the study volume. The monofractal distribution used here (code provided by A. Davis, private communication) is characterized by a fractal dimension 2.35. The point co-ordinates in this case are generated by using the mid-point displacement algorithm to simulate fractional Brownian motion with exponent 1/2.35. The particular choice of the value 2.35 will be explained below.

The volume in which the random points are generated is determined by the real data; that is, this volume is of irregular shape and covers closely the real Data Set 2. This is achieved by randomly generating points in a parallelepiped encompassing the real data, but retaining only the points that fall within a prescribed distance from the real events. The distance used here, 15 m, is comparable to the location error. Although this procedure introduces additional geometric structure into the cloud of randomly distributed points, it most adequately reflects the fact that the volume covered by the real data might contain non-negligible "holes" inside. The resolution with which one has to account for such effects is obviously disputable. As the distance used to construct the irregular volume increases, the spreading pattern seen in the family of generalized correlation integrals shrinks. It is to be noted, however, that the generalized correlation integrals for a volume with regular shape and no inner geometric complexity (not shown here), still exhibit a spreading pattern (i.e., spurious multifractality), although to a lesser extent. Since the spreading observed in Figs.3b and 3c can be only due to the use of limited data sets in terms of size and geometry of the study volume, and/or number of events, the appearance of the generalized correlation integrals for the real data in Fig.3a cannot be reliably considered as a sign of multifractality. It will be shown later that some types of limitations may have a stronger effect than other types.

4.2 Choice of scaling range

The method used here to evaluate the dimensions $D^{(q)}$ consists of calculating the slopes of the straight segments of the integrals from Fig.3. The intent is to avoid the edge effects appearing in the correlation integrals for too small or too large distances. More often than not, it is not being particularly discussed in the literature how these straight segments are chosen. One of three methods can

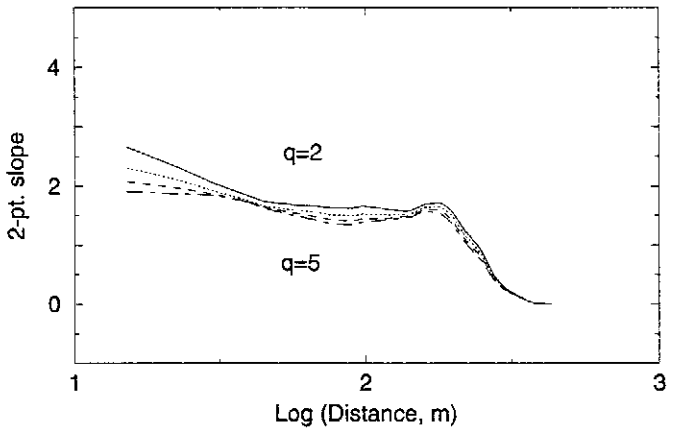

Fig.4. Two-point slopes estimated from the generalized correlation integrals for integer values $2 \leq q \leq 5$.

be used: (1) choosing arbitrary segments which are visibly straight (most frequently used by authors); (2) calculating the slopes for each two consecutive points of a given generalized correlation integral and choosing the distance range over which the two-point slopes do not vary significantly; and (3) introducing some formalism to evaluate the "proper" straight segment for a given data set.

One example of the third method applied in the case of $D^{(2)}$ is the work of Nerenberg and Essex (1990). They determine two characteristic distances, the distance of depopulation (r_n) and the distance of saturation (r_s), as functions of the embedding dimension (d), the number of points (N), and the linear size (2R) of the hypercube encompassing the data set: $r_n = 2R(1/N)^{1/d}$ and $r_s = R/(d+1)$. It is to be noted in these estimates that the saturation distance (r_s) depends on the size of the volume (2R) and the embedding dimension (d), but not on the number of points (N). Thus, using more data points extends the scaling range only at the lower end; i.e., for small distances. A proper scaling region is the one between distances r_n and r_s. If $r_s < r_n$ for a particular data set, a proper scaling region cannot be defined. In practical applications, it is safe to start the scaling range quite below r_n (for example, at $r_n/3$). The role of r_s, however, is more decisive. In practice, the correlation integrals do not necessarily bend at the distance of saturation. Reasonable straight segments can be observed for distances significantly larger than r_s. The estimates of the correlation dimension evaluated over the whole visible straight segment is then quite low, as significant saturation is already involved. Thus, a proper scaling range is not necessarily identical with the distance range over which the best straight segment from a statistical point of view can be defined (see (1) and (2) above).

Figure 4 shows examples of two-point slopes calculated from the generalized correlation integrals as functions of distance for the real Data Set 2. Similar curves were evaluated for the random data sets as well (not shown). Figure 4 is representative for other values of $q \geq 0$ as well; in fact, the variability for $q > 5$ (not shown) is even less noticeable. This plot indicates that a reasonably good scaling range from a statistical point of view is the one over distances 30-120 m (1.5-2.1 in log-scale). This is the range used further to evaluate $D^{(q)}$ for $q \geq 0$. In contrast, the variability of the two-point slopes for $q < 0$ is very large and these are not considered further.

To see how the range chosen above (30-120 m) compares with the proper scaling range, the formalism described by Nerenberg and Essex (1990) is applied to the specific case studied here. The following values are used: $d = 3$; $N = 1654$; and 2R falling between 180 and 400 m for the initially imposed volume. Note that 2R is smaller for the effective volume. If one considers the proper range for the practical evaluation of $D^{(2)}$ to be between $r_n/3$ and r_s, a range 1-23 m at least and 3-50 m at most is obtained.

There is, however, an additional parameter to be seriously considered here: the location error. It does not make sense to either consider distances smaller than this error or attempt to distinguish between points of the correlation integral spaced more closely than the error. This leaves us with a proper scaling range 15-50 m at best, over which one can only consider points of the integral evaluated for distances 15 m or more apart. There are at least two arguments, however, that point to the necessity for a larger distance to be used as a lower limit of the scaling region. First, from statistical point of view, 15 m (or 1.2 in the log scale of Fig.4) is already outside the relatively flat portions of the two-point slope curves. Second, given that 15 m is representative for the location error here, it is wise to consider the beginning of the straight segments at a larger distance, following the estimates made by Kagan and Knopoff (1980) for the radius of influence of the location error of earthquake hypocentres. Thus, 30-50 m may be a more appropriate range than 15-50 m, although it is too short to be practically useful. As indicated above, the range 30-120 m appears a reasonable choice from a statistical point of view, although it is much wider than the presumed proper range. Obviously, if we insist on either using the proper range or not performing any analysis, not much choice is left and valuable information has to be dropped.

No theoretical frame (like the one described for $q = 2$ by Nerenberg and Essex, (1990)) is available to estimate the proper ranges for values of $q \neq 2$, but similar to the case of $D^{(2)}$, we can assume that these ranges are shorter than the distance ranges over which statistically good straight segments are observed. Nonetheless, it is possible to proceed with using the range 30-120 m for all $q \geq 0$; this does result in low values for the dimensions, but the bias can be readily evaluated through comparison with the effect on randomly generated points scattered according to known distributions. The term "bias" here is not to be understood by analogy with standard deviations, for

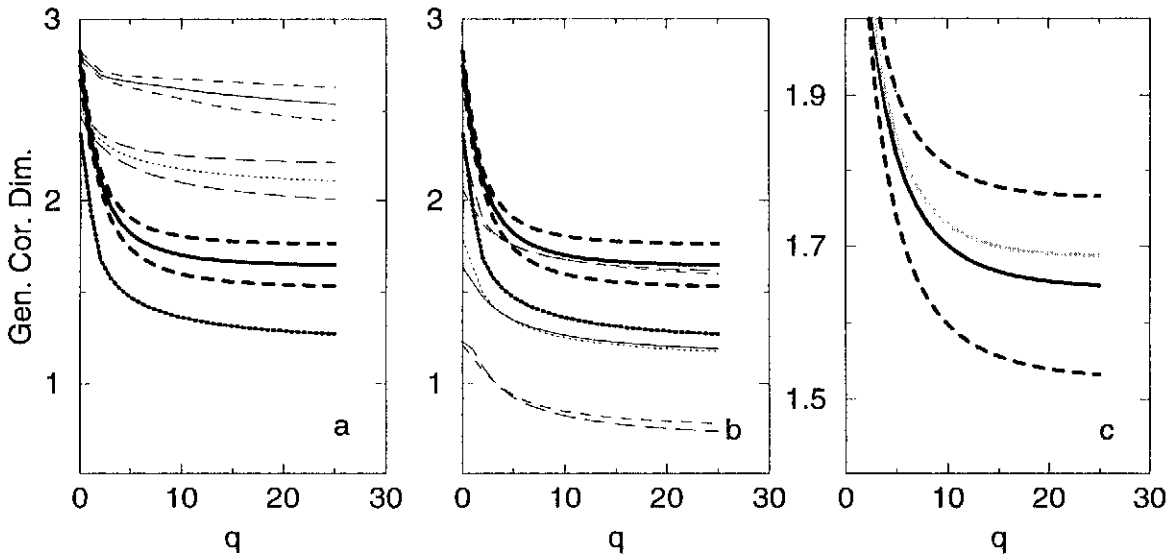

Fig.5. Spectra of dimensions ($q \geq 0$) for Data Set 1 and Data Set 2 (all bold lines) shown together with the average $\pm$ 2 standard deviations of the spectra obtained from randomly simulated sets of 1654 points each (all thin lines), using a uniform (a) and monofractal (b) distributions. Dotted bold line in (a) and (b) - $D^{(q)}$-spectrum for Data Set 2. Solid and dashed bold lines in all frames - mean $\pm$ 2 st. dev. estimated for 100 samples from Data Set 1 (1654 events each). Grey bold line in (c) - spectrum for the whole Data Set 1 (14,338 events). Thin solid and dashed lines in (a) and (b) - mean $\pm$ 2 st. dev. estimated from 50 randomly simulated sets of points in the volume of Data Set 1. Thin dotted and long-dash lines in (a) and (b) - same, but for the volume of Data Set 2.

example. It represents in fact a one-sided bias that only leads to lower estimates, unlike standard errors equally likely to result in measurements above or below estimated means.

It is to be noted that, in principle, correlation integrals like the ones in Fig.3 above, reflect the combined effect of the fracture process and the artificial inhomogeneity imposed by the excavation, the blasting, and the geometry of the mine openings. Thus, significant non-linearities in the proper scaling range would not necessarily indicate a lack of scaling in the seismic process. The mine openings, however, are unlikely to have any effect here, as their diameters are much smaller than the lower limit of 30 m used in the present work. The inhomogeneities due to the excavation and the blasting are potentially much more important, but no significant non-linearities are observed within the scaling range chosen here.

4.3 Comparison of Data Sets 1 and 2

The generalized correlation integrals shown in each of Figs.3b and 3c above were calculated from a single set of simulated points. Thus, a single dimension spectrum corresponds to each of these families of curves. It is, however, unacceptable to compare the spectra for the real data sets with isolated randomly generated point sets. For this reason, 50 point sets are simulated in each case, resulting in 50 simulated spectra. The average $\pm$ 2 standard deviations of those are used for comparison with the spectra for the real data.

Similar computations are performed for Data Set 1 as for data Set 2 above, using the same scaling range 30-120 m. Figure 5 compares results from Data Sets 1 and 2. Several issues need to be addressed before this comparison is performed. First, recall that although both data sets were initially extracted using the same imposed volume, the effective volumes covered by the two data sets are different. For this reason, the volumes used for the random generations are different, as in each case the randomly generated points were compared with the respective real event locations and only the ones within 15 m from them were retained. Second, in order to compare the two data sets, one should initially use the same numbers of events. Thus differences, if any, would not be due to the use of different numbers of events. For this reason, while a single $D^{(q)}$-spectrum is used for Data Set 2 (1654 events), 100 $D^{(q)}$-spectra are calculated for Data Set 1 instead of using all events (14,338) at once. The latter is done by re-sampling the real Data Set 1, so that 100 samples of 1654 events each (same number as in Data Set 2) are randomly extracted from Data Set 1. Thus, the real Data Set 1 is not represented by a single spectrum, but by the average $\pm$ 2 standard deviations, obtained from these 100 samples. The random re-sampling of real data here is not to be confused with the random simulations. As the procedure of re-sampling is faster than the random simulations, 100 samples from Data Set 1 were used versus only 50 random simulations.

Figure 5a shows the $D^{(q)}$-spectra for the real Data Set 2 (a single spectrum) and Data Set 1 (average spectrum $\pm$ 2 st. deviations from re-sampling), together with results from 50 randomly generated sets of 1654 points each (average $\pm$ 2 st. deviations from random simulations). If the data sets were not limited, the spectra for the random data would have been represented by horizontal lines through values around 3 (since the embedding dimension

is d=3). Figure 5b shows the same as Fig.5a, but the random simulations use monofractal distributions with fractal dimensions 2.35 and 2.40 for Data Set 2 and Data Set 1, respectively. Finally, Fig.5c displays only results for Data Set 1, showing again the real $D^{(q)}$-spectra calculated from the re-sampling (1654 events per sample), together with the $D^{(q)}$-spectrum calculated from the whole Data Set 1 (14,338 events).

Figure 5a first suggests that the $D^{(q)}$-spectra for the real data is significantly different from the "spuriously multifractal" spectra for the uniform random points. It is apparent that the generalized correlation dimensions for the random data are all lower than 3 and the bias is larger for the random simulations in the volume of Data Set 2. This is entirely due to the fact, that this volume is at most 85% of the volume for Data Set 1; i.e., the effect of changing size of effective volume (and not number of simulated events) is demonstrated here very well. Second, Fig.5a shows that there is a significant difference between the spectra for the two real data sets. Since it is not due to differences in the number of events used, it can be only attributed to two other factors: differences in the volumes occupied by the two data sets and/or real differences between larger (Data Set 2) and smaller (Data Set 1) microearthquakes. The first of this factors is apparently responsible for most, if not all, of the discrepancy, as the offset between the random spectra (due only to difference in volume sizes) is approximately the same as the offset between the spectra for the real data sets. Thus, a significant difference between smaller and larger microearthquakes is unlikely to exist in this respect, despite the appearance of the $D^{(q)}$-spectra. All this shows that unless comparisons with simulated data are performed, one cannot reliably distinguish between the scaling properties of data sets filling in volumes of different size and geometry.

Figure 5b suggests that although different from uniform random distribution (Fig.5a), the spatial distribution of the microearthquakes in Data Set 2 apparently cannot be shown to be genuinely multifractal. No significant difference can be demonstrated between the real spectrum for this data set and the simulated spectra. The spectra from the monofractal distributions almost overlap, leaving the real $D^{(q)}$-spectrum for Data Set 1 high up. However, higher values for the fractal dimension in the random generations are expected to raise the simulated spectra further up, enough to substantially include larger portions of the spectra for the real data. Thus, at most, only weak multifractality can be assumed for Data Set 1 (for $q<5$). Note that the scatter of the $D^{(q)}$-spectra is about 3 times larger for the monofractal simulations than for the uniform ones (compare the bands outlined by 2 standard deviations in Figs.5a and 5b).

The value 2.35 for the fractal dimension of the simulated monofractal distribution in the volume of Data Set 2 above was chosen for the following reasons. Various tests with the algorithm generating monofractals with a prescribed fractal dimension indicated that a very good estimate of this dimension is provided by the correlation dimension $D^{(2)}$ (given that a proper scaling region is used). On the other hand, the estimate of $D^{(2)}$ over distances 30-120 m is 1.68 for Data Set 2. The values of $D^{(2)}$ estimated over the same range for 50 sets of 1654 points each, randomly generated within the irregular volume, using uniform distribution, vary between 2.31 and 2.38. These latter values, compared with the proper value of 3, indicate that the correlation dimensions for the uniform random points are by 0.62 to 0.69 lower for the specific limited data set used here. If an error of the same order is committed when the correlation dimension is evaluated for the real data set, and if it were a monofractal, one can assume that its "true" dimension is somewhere between $1.68+0.62=2.30$ and $1.68+0.69=2.37$. Thus, a value of 2.35 seemed to be a reasonable first choice for the prescribed fractal dimension in generating the random monofractal. Upon further consideration, however, the choice of the fractal dimension for the monofractal simulation may not be that simple, as the error committed with the uniform random distributions is probably only a lower bound of the bias for other distributions. For example, $D^{(2)}=1.49\pm0.40$ for the monofractal simulations in Fig.5b, which indicates a bias of $2.35-(1.49\pm0.40)=0.86\pm0.40$. Thus, one might have to extensively experiment with various monofractals of fractal dimensions > 2.35, which is not done in this work. In view of the wide spread of the simulated spectra here, it is expected that reasonably higher values of the fractal dimension in the simulations would still not result in demonstrating genuine multifractality for the real Data Set 2.

Following the same reasoning as for Data Set 2, the fractal dimension used for the simulations in the volume of Data Set 1 was chosen as $2.40=2.11+0.29$. This latter value was estimated taking into account the value of the average correlation dimension, $D^{(2)}=2.11$ (from 100 randomly chosen samples), and the range obtained for randomly and uniformly generated points, 2.68 to 2.72, suggesting a bias of 0.28-0.32. This bias is naturally smaller than the bias for the random points in the volume of Data Set 2 (0.62-0.69), as the effective volumes covered by the two data sets are of different size. Obviously, the difference between the simulated spectra obtained using fractal dimensions 2.35 (for Data Set 2) and 2.40 (for Data Set 1) is negligible, despite the difference in the effective volumes.

Finally, Fig.5c demonstrates that using almost an order of more events (14,338) still results in a spectrum that is very similar to the sample spectra (for 1654 events each), only slightly above the average spectrum. This is not surprising in view of the fact that increasing number of events only extends the scaling range at the lower end (for small distances) of the correlation integrals. One cannot

really take advantage of such an improvement in the case studied here, as the location error (of the order of 15 m) puts the lower bound at much higher distances.

5 Conclusions

The strong appearance of multifractal features in the global scaling properties of the spatial distribution of mining induced seismic activity in Creighton Mine (northern Ontario) is largely spurious in character. Analysis of the limitations associated with the data sets studied shows that this distribution can be either described by only a weak multifractal (particularly for the smaller events) or a monofractal with a dimension probably not lower than 2.35. Similarly, multifractals used in the literature, might have been inappropriate in some cases if the effect of finite data sets is not evaluated.

In both the monofractal and the multifractal cases, comparisons of values of fractal dimensions estimated from data sets featuring different numbers of events, different measurement errors, different geometries of the embedding space, and different scaling ranges, seem to be particularly wrong. The spurious features may be predominant in such comparisons and differences likely to reflect real physical processes cannot be established without additional considerations.

In this connection, a very popular, but questionable, approach is to give a particular meaning of the estimated fractal dimensions between 1 and 2 or 2 and 3 as indicating different degrees of space or volume filling properties. A data set with volume filling properties, however, can easily be misrepresented as space filling. For example, the estimated value for $D^{(2)}$ is below 2 for Data Set 2 in this study, while $D^{(2)}>2$ for Data Set 1. If the artifacts of working with data sets that are subject to different limitations are not taken into account, one can reach wrong conclusions about fundamental differences between smaller and larger events. Indeed, it was shown in the present work, that this difference is mainly due to the difference in the sizes and/or geometries of the effective volumes covered by the two data sets.

Comparison with results from randomly generated point sets using known distributions (such as uniform and monofractal), appear to be an effective way to estimate the bias introduced by the limitations of the real data. In addition, the effect of limited number of events in particular, can be evaluated by re-sampling the real data, extracting at random samples of the desired number of events. When compared with the dimensions evaluated from the whole data set, these show that improvement in estimates is very slow with increasing numbers of events. Increasing number of events improves only the lower end of the scaling range, i.e., for small distances. If this is in conflict with the measurement error (location error here), i.e., the radius of influence of the error is larger than the proper distance of depopulation, increasing the number of events remains without any effect. This indicates that instead of attempting to work with ever increasing numbers of data, a better approach may be to find ways to evaluate the bias introduced by the particular limitations of the data sets studied. In fact, in many fields, collecting a large number of observations would pose an unsurmountable problem, let alone the amount of computer time needed.

The above possibility to effectively work with small data sets allows us to split the real data into overlapping groups of events and evaluate the temporal changes of the scaling properties, if any. Decreasing correlation dimensions, indicative for increasing spatial clustering, might be of particular interest, as Hirata (1989), Coughlin and Kranz (1991), and Eneva and Young (1993) among others, have reported such trends before larger earthquakes and larger events in mines. More generally, decreasing fractal dimensions appear to precede various phenomena that can be described as "catastrophes", such as tropical cyclones (Moiseev, private communication). Isolated observations, however, are not sufficient and further studies along this line are called for.

The present work concentrated only on the slope method of estimating the generalized correlation dimensions, as this method is very widely, and sometimes, indiscriminately, used. The slope method has been criticised by Wells et al.(1994) (see numerous references therein) who devise an integral method to avoid the assumption that the correlation integral (for $q=2$) is always differentiable. It appears that their method can be easily extended to the remaining generalized dimensions ($q\neq 2$). The estimates made using methods different from the slope method (e.g., Tessier et al., 1993) may be conceptually less prone to large biases. It appears, however, that comparison with randomly generated point sets mimicking the limitations of the real data would be always informative and illuminating.

Aknowledgments. This study has been funded by Inco Ltd., Sudbury, Ontario (Canada). Numerous discussions with Doug Morrison and Terry Villeneuve from Inco Ltd. substantially helped me to understand the peculiarities of the data featuring mining induced seismic activity. I am greatly indebted to Anthony Davis from NASA/GSFC for providing the program for generating monofractal distributions, as well as for the numerous discussions on the subject. I thank Anthony Davis and Yan Kagan for reviewing the initial manuscript and providing valuable suggestions for its improvement. Finally, I highly appreciate the feedback and suggestions I got from the participants in the Chapman Conference on Nonlinear Variability in Geophysics, September 1993.

References

Aki, K., A probabilistic synthesis of precursory phenomena, in *Earthquake Prediction, AGU, Maurice Ewing Series 4*, Simpson, D.W. and Richards, P.G., eds., 566-574, 1981.

Atmanspacher, H., Scheingraber, H., and Voges, W., Global scaling properties of a chaotic attractor reconstructed from experimental data, *Phys. Rev., 37A*, 1314-1322, 1988.

Aviles, C.A. and Scholz, C.H., Fractal analysis applied to characteristic segments of the San Andreas fault, *J. Geophys. Res., 92*, 331-344, 1987.

Block, A., von Bloh, W., Klenke, T., and Schellnhuber, H.J., Multifractal analysis of the microdistribution of elements in sedimentary structures using images from scanning electron microscopy and energy dispersive X ray spectrometry, *J. Geophys. Res., 96*, 16223-16230, 1991.

Coughlin, J. and Kranz, R., New approaches to studying rock burst-associated seismicity in mines, in *Proc. 32nd U.S. Symp., Rock Mechanics as a Multidisciplinary Science*, Roegiers, J.-C., ed., 491-500, 1991.

Davy, P., Sornette, A., and Sornette, D., Experimental discovery of scaling lows relating fractal dimensions and the length distribution exponent of fault systems, *Geophys. Res. Lett., 19*, 361-363, 1992.

Eneva, M., *Investigation of the space-time distribution of earthquakes in the Charlevoix seismic zone*, Quebec, Open-File Report, Geological Survey of Canada, Ottawa, in press.

Eneva, M., Hamburger, M.W., and Popandopulo, G.A., Spatial distribution of earthquakes in aftershock zones of the Garm region, Soviet Central Asia, *Geophys. J. Int., 109*, 38-53, 1992.

Eneva, M. and Young, R. P., Evaluation of spatial patterns in the distribution of seismic activity in mines: A case study of Creighton Mine, northern Ontario (Canada), in *Rockbursts and seismicity in mines*, Young, R. P., ed., A. A. Balkema Publ., 175-180, 1993.

Ge, M. and Kaiser, P.K., Interpretation of physical status of arrival picks for microseismic source location, *Bull. Seism. Soc. Am., 80*, 1643-1660, 1990.

Grassberger, P., Generalized dimensions of strange attractors, *Phys. Lett., 97A*, 227-230, 1983.

Grassberger, P. and Procaccia, I., Characterization of strange attractors, *Phys. Rev. Lett., 50*, 346-349, 1983.

Halsey, C., Jensen, M. H., Kadanoff, L. P., Procaccia, I., Shraiman, B. I., Fractal measures and their singularities: The characterization of strange sets, *Phys. Rev., 33A*, 1141-1151, 1986.

Henderson, J. and Main, I., A simple fracture-mechanical model for the evolution of seismicity, *Geophys. Res. Lett, 19*, 365-368, 1992.

Hentschel, H. G. E. and Procaccia, I., The infinite number of generalized dimensions of fractals and strange attractors, *Physica, 8D*, 435-444, 1983.

Hirata, T., A correlation between the b value and the fractal dimension of earthquakes, *J. Geophys. Res., 94*, 7507-7514, 1989.

Hirata, T. and Imoto, M., Multifractal analysis of spatial distribution of microearthquakes in the Kanto region, *Geophys. J. Int., 107*, 155-162, 1991.

Kagan, Y. and Knopoff, L., Spatial distribution of earthquakes: the two-point correlation function, *Geophys. J. R. astr. Soc., 62*, 303-320, 1980.

Kurths, J. and Herzel, H., An attractor in a solar time series, *Physica, 25D*, 165-172, 1987.

Lovejoy, S. and Schertzer, D., Our multifractal atmosphere: A unique laboratory for non-linear dynamics, *Physics in Canada, 46*, 62-71, 1990.

Main, I., Damage mechanics with long-range interactions: correlation between the seismic b-value and the fractal two-point correlation dimension, *Geophys. J. Int., 111*, 531-541, 1992.

Marshak, A., Davis, A., Cahalan, R., and Wiscombe, W., Bounded cascade models as nonstationary multifractals, *Phys. Rev. E*, in press, 1993.

Morrison, D. M. and MacDonald, P., Rockbursts at Inco mines, in *Proceedings of the 2nd International Symposium on Rockbursts and Seismicity in Mines, Mineapolis 8-10 June 1988*, Fairhurst, C., ed., 263-267, 1990.

Nerenberg, M. A. H. and Essex, C., Correlation dimension and systematic geometric effects, *Phys. Rev., 42A*, 7065-7074, 1990.

Pawelzik, K. and Schuster, H. G., Generalized dimensions and entropies from a measured time series, *Phys. Rev., 35A*, 481-484, 1987.

Rundle, J.B., Derivation of the complete Gutenberg-Richter magnitude-frequency relation using the principle of scale invariance, *J. Geophys. Res., 94*, 1273-12342, 1989.

Tessier, Y., Lovejoy, S., and Schertzer, D., Universal multifractals: Theory and observations for rain and clouds, *J. Appl. Meteor., 32*, 223-250, 1993.

Turcotte, D.L., A fractal model for crustal deformation, *Tectonophysics, 132*, 261-269, 1986.

Wells, R., Shirer, H.N., Fosmire, C.J., Doran, J.A., Improved algorithms for estimating the correlation dimension and the associated probable errors, *Physica D*, in press.